



ARL-CR-0865 • Nov 2021



# The Gleeble as a Tool for High-Throughput Materials Discovery

by Franklyn Kellogg  
*SURVICE Engineering*  
4687 Millennium Drive, Belcamp, MD

under contract W15P7T-19-D-0126

Approved for public release: distribution unlimited.

## **NOTICES**

### **Disclaimers**

The findings in this report are not to be construed as an official Department of the Army position unless so designated by other authorized documents.

Citation of manufacturer's or trade names does not constitute an official endorsement or approval of the use thereof.

Destroy this report when it is no longer needed. Do not return it to the originator.



# The Gleeble as a Tool for High-Throughput Materials Discovery

by Franklyn Kellogg  
*SURVICE Engineering*  
*4687 Millennium Drive, Belcamp, MD*

under contract W15P7T-19-D-0126

**REPORT DOCUMENTATION PAGE**

*Form Approved  
OMB No. 0704-0188*

Public reporting burden for this collection of information is estimated to average 1 hour per response, including the time for reviewing instructions, searching existing data sources, gathering and maintaining the data needed, and completing and reviewing the collection information. Send comments regarding this burden estimate or any other aspect of this collection of information, including suggestions for reducing the burden, to Department of Defense, Washington Headquarters Services, Directorate for Information Operations and Reports (0704-0188), 1215 Jefferson Davis Highway, Suite 1204, Arlington, VA 22202-4302. Respondents should be aware that notwithstanding any other provision of law, no person shall be subject to any penalty for failing to comply with a collection of information if it does not display a currently valid OMB control number.

**PLEASE DO NOT RETURN YOUR FORM TO THE ABOVE ADDRESS.**

<b>1. REPORT DATE (DD-MM-YYYY)</b> November 2021		<b>2. REPORT TYPE</b> Contractor Report		<b>3. DATES COVERED (From - To)</b> 01 June–01 Sept 2021	
<b>4. TITLE AND SUBTITLE</b> The Gleeble as a Tool for High-Throughput Materials Discovery				<b>5a. CONTRACT NUMBER</b> W15P7T-19-D-0126	
				<b>5b. GRANT NUMBER</b>	
				<b>5c. PROGRAM ELEMENT NUMBER</b>	
<b>6. AUTHOR(S)</b> Franklyn Kellogg				<b>5d. PROJECT NUMBER</b>	
				<b>5e. TASK NUMBER</b>	
				<b>5f. WORK UNIT NUMBER</b>	
<b>7. PERFORMING ORGANIZATION NAME(S) AND ADDRESS(ES)</b> SURVICE Engineering 4687 Millennium Drive Belcamp, MD 21017				<b>8. PERFORMING ORGANIZATION REPORT NUMBER</b>	
<b>9. SPONSORING/MONITORING AGENCY NAME(S) AND ADDRESS(ES)</b> DEVCOM Army Research Laboratory ATTN: FCDD-RLW-MD Aberdeen Proving Ground, MD 21005				<b>10. SPONSOR/MONITOR'S ACRONYM(S)</b>	
				<b>11. SPONSOR/MONITOR'S REPORT NUMBER(S)</b> ARL-CR-0865	
<b>12. DISTRIBUTION/AVAILABILITY STATEMENT</b> Approved for public release: distribution unlimited.					
<b>13. SUPPLEMENTARY NOTES</b> ORCID ID: Franklyn Kellogg, 0000-0003-3048-0255					
<b>14. ABSTRACT</b> This report is intended to provide an example-based understanding of how a Gleeble thermal–mechanical physical process simulator can contribute to alloy development via a High-Throughput Materials Design approach. Typically, a Gleeble is not considered high throughput because it only outputs one test result per sample; that is, you can only perform one mechanical test or one rolling simulation per sample. However, through the application of thermal gradients a Gleeble can create many different and distinct microstructures within one sample during one test. This report presents a quick demonstration of the steps needed to develop a microstructural library using 1018 steel as an example material.					
<b>15. SUBJECT TERMS</b> High-Throughput Materials Design, Gleeble, 1018 steel, physical simulation, microstructural library					
<b>16. SECURITY CLASSIFICATION OF:</b>			<b>17. LIMITATION OF ABSTRACT</b> UU	<b>18. NUMBER OF PAGES</b> 24	<b>19a. NAME OF RESPONSIBLE PERSON</b> Franklyn Kellogg
<b>a. REPORT</b> Unclassified	<b>b. ABSTRACT</b> Unclassified	<b>c. THIS PAGE</b> Unclassified			<b>19b. TELEPHONE NUMBER (Include area code)</b> (410) 306-0803

## **Contents**

---

<b>List of Figures</b>	<b>iv</b>
<b>List of Tables</b>	<b>iv</b>
<b>Acknowledgments</b>	<b>v</b>
<b>1. Introduction</b>	<b>1</b>
<b>2. Experimental</b>	<b>3</b>
<b>3. Results</b>	<b>5</b>
<b>4. Conclusions</b>	<b>14</b>
<b>5. References</b>	<b>15</b>
<b>List of Symbols, Abbreviations, and Acronyms</b>	<b>16</b>
<b>Distribution List</b>	<b>17</b>

## List of Figures

---

Fig. 1	Schematic of the “Valley of Death” .....	1
Fig. 2	Cu (A) and steel (B) Gleeble grips for 10-mm-diameter samples, and highlighted red regions (C) are the contact area for each grip; ruler is in inches .....	3
Fig. 3	Sample using Cu grips with TCs welded on, ready to load into Gleeble .....	4
Fig. 4	Sample using Cu grips loaded into Gleeble .....	4
Fig. 5	Measured temperature profiles for Samples 1–4; Sample 2 had smallest thermal gradient while Sample 3 had largest.....	6
Fig. 6	Measured maximum temperatures for each TC for samples tested with the Cu grips (Samples 1, 3, 5, and 6) as a function of distance from stationary end of Gleeble .....	7
Fig. 7	Measured maximum temperatures for each TC for samples tested with steel grips (Samples 2 and 4) as a function of distance from stationary end of the Gleeble .....	7
Fig. 8	Gleeble heat power (power output) as a function of time overlaid on the programmed thermal profile, as controlled by TC 2, for Samples 3, 5, and 6 run with the Cu grips, no hold time, and heating rates of 5, 10, and 20 °C/s.....	8
Fig. 9	Maximum temperature measured by each TC for Sample 3 as function of distance away from control thermocouple (TC2 taken as $x = 0$ ) ...	10
Fig. 10	Low-magnification image of Sample 3 after metallographic preparation showing where in the sample the TCs were attached and where the higher-magnification images (Figs. 11–14) were taken.....	10
Fig. 11	Higher-magnification images of Sample 3 .....	11
Fig. 12	Blown-up versions of middle images in Fig. 11: yellow boxes block off precipitates seen throughout the sample while red circles are example areas of pearlite .....	11
Fig. 13	High-magnification images showing differences in the pearlite throughout sample.....	12
Fig. 14	High-magnification images showing the precipitates in Fig. 12 .....	12
Fig. 15	Iron–carbon phase diagram; red line roughly indicates carbon content in 1018 steel .....	13

## List of Tables

---

Table 1	Experimental parameters and measured thermal gradients; highlighted row is sample that had largest thermal gradient.....	5
---------	--	---

## **Acknowledgments**

---

The research reported in this report was performed in connection with contract/instrument W15P7T-19-D-0126 with the US Army Combat Capabilities Development Command (DEVCOM) Army Research Laboratory (ARL). The views and conclusions contained in this document are those of SURVICE Engineering and the DEVCOM Army Research Laboratory. Citation of manufacturer's or trade names does not constitute an official endorsement or approval of the use thereof. The US government is authorized to reproduce and distribute reprints for government purposes notwithstanding any copyright notation hereon.

Special thanks to Drs Clara Mock and Dan Field of DEVCOM ARL for their help with the metallography and microscopy.

## 1. Introduction

---

Historically, it has taken approximately 20 years to advance a material from discovery to final product.<sup>1</sup> This 20-year gap is often referred to as the “Valley of Death” as most laboratory discoveries never make it to commercialization.<sup>2</sup> The valley has many causes and factors that make it grow (for example: technical issues, operational costs, and regulations) but relatively few tools available to shrink it (Fig. 1).

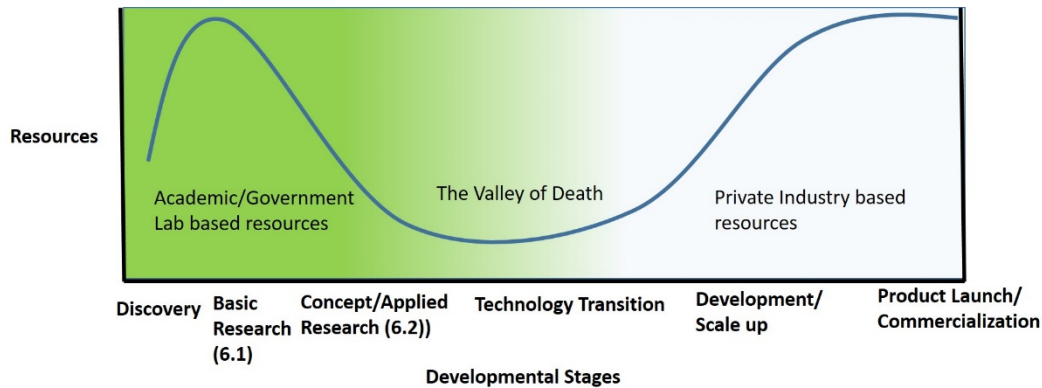


Fig. 1 Schematic of the “Valley of Death”

As the need for the development of new materials to solve global problems grows, it becomes imperative to shrink the valley to a much more manageable time frame. Shrinking the valley is the main driving force in creating the framework of High-Throughput Materials Development (HTMD).

One strategy for HTMD is to break the entire materials-discovery process down to a few broad steps: *Materials Discovery* (identifying a needed and desired property of a given material), *Knowledge Discovery* (finding relationships within the material composition; for example, iron and carbon in a steel), the formation of *Discrete Libraries* (uniform distinct compositions), the formation of *Gradient Libraries* (one composition but with different microstructures), and *Experimental* measurements to determine properties and material behavior.<sup>3</sup> The overarching idea for HTMD is to get as much data, relevant to the desired properties of the end need, in as few tests and with as little material as possible. For this report, the focus is going to be on Step 4: the formation of gradient libraries.

Once a material composition has been decided upon, the next step is to find which microstructure gives the desired properties and behavior. When dealing with metal alloys, there are two ways to develop any microstructure: through the application of thermal (heat) energy and/or the application of mechanical (work) energy.<sup>3</sup> For forming a gradient library, it is best to separate the contributions of both energy



inputs. A thermal gradient library is formed when a sample is subjected to a temperature gradient at a constant load, while a strain gradient library is formed when a sample is held at a constant temperature but undergoes nonuniform deformation (an imposed strain gradient). In both cases, the end goal is to produce as many individual and distinct microstructures as possible within a single sample during one test. A Gleeble physical process simulator can easily generate both types of gradient libraries, although the focus of this report is on the formation of thermal gradient libraries.

A Gleeble system (Dynamic Systems, Inc. [DSI]) is designed to, through the application of heat and strain, physically simulate virtually any type of metals-forming process. One of the key attributes of the Gleeble is it can heat metallic samples to very high temperatures (3000 °C) very rapidly (up to 10,000 °C/s). The Gleeble accomplishes this by the application of large amounts of AC current across a sample, where the resistance of the sample to the current flow causes the sample to heat up. One of the drawbacks of resistance heating is this normally leads to very large thermal gradients along the length of the sample (but negligible thermal gradients along the radius of the sample). During conventional Gleeble simulations, thermal gradients are managed through either sample geometry or test setup (primarily Gleeble grip selection).<sup>4</sup>

Long samples with a small diameter experience the largest gradients, while samples with either larger diameters and/or shorter lengths or with a smaller diameter (relative to the rest of the sample) gauge section—for example, a dog-bone shaped sample—experience smaller thermal gradients.

Another way to control the current flow through a sample within the Gleeble is to change the grip material (Fig. 2). To achieve the highest heating rates, the Gleeble uses copper (Cu) grips because of Cu's very high thermal and electrical conductivity. However, the very high thermal conductivity of Cu also ensures the ends of the sample are rapidly cooled and this increases the thermal gradient across the sample. The steel grips in Fig. 2B are also known as “hot jaws” and are specially designed to be less conductive through material choice (steel is less conductive than Cu) and by design: The steel grips are designed to have less contact area with the sample than the Cu grips and have holes machined into them to further limit their conductivity.

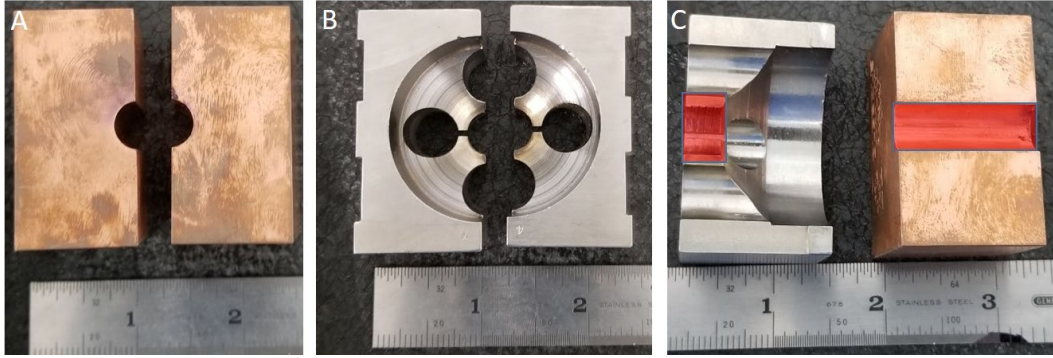


**Fig. 2** Cu (A) and steel (B) Gleeble grips for 10-mm-diameter samples, and highlighted red regions (C) are the contact area for each grip; ruler is in inches

While the thermal gradients, during traditional tests, must be controlled to ensure a uniform sample microstructure during testing, the exact opposite is true when the goal is to develop a microstructural library. For forming microstructural libraries, the largest gradients possible are desired to generate the most microstructures possible in the fewest number of tests. In this report, the effects of grip choice, hold time, and heating rate on the size of the thermal gradient generated and the resulting variations in microstructure after cooling were investigated. The material of choice for these experiments was 1018 steel. The 1018 is a commonly used low-carbon steel (0.18–0.20% carbon, 0.60–0.90% manganese with iron as the balance)<sup>5</sup> that was chosen for these experiments due to availability and ease of use.

## 2. Experimental

---

The 10-mm-diameter by 141-mm-long (50-mm-long gauge section) 1018 steel cylinders were provided by DSI when they installed the Gleeble 3800 at the US Army Combat Capabilities Development Command Army Research Laboratory. Each cylinder was lightly scrubbed with a Brillo pad to remove surface rust and scale. K-type thermocouple leads were then percussion-welded to the sample to create four thermocouples. In each sample, the thermocouples (TCs) were tracked as TC1, TC2, TC3, and TC4 (Fig. 3). TC1 was the thermocouple nearest to the moving grip in the Gleeble (Fig. 4) while TC2 was always in the middle of the sample. The Gleeble was told to use TC2 to measure the sample temperature and control heating while TC1, TC3, and TC4 were used only to monitor and record temperature data. Because TC2 is the control thermocouple, it always read the highest temperature in these experiments. TC3 was 5 to 10 mm to the right of TC2 (between TC2 and TC4), while TC4 was always the thermocouple nearest to the grip on the stationary end. TCs 1 and 4 were always 5 to 7 mm away from the nearest contact point between the Cu grips and the sample. For the steel grips, TCs 1 and 4 were always 5 to 7 mm away from the outermost edge of the grip. Due to

the reduced contact area of the steel grips, this ended up being approximately 25 mm from the contact point between the grips and the sample. After welding, alumina wire guards were slid down the leads and over the bare wire, making the thermocouple junctions to prevent the wires from contacting one another and shorting out. The sample was then loaded into the Gleeble.

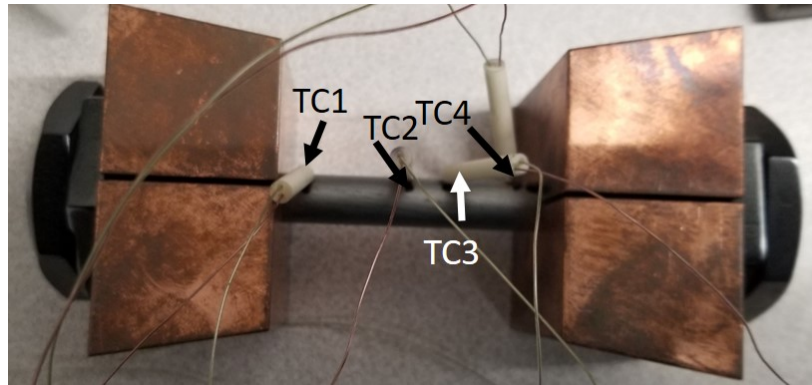


**Fig. 3** Sample using Cu grips with TCs welded on, ready to load into Gleeble

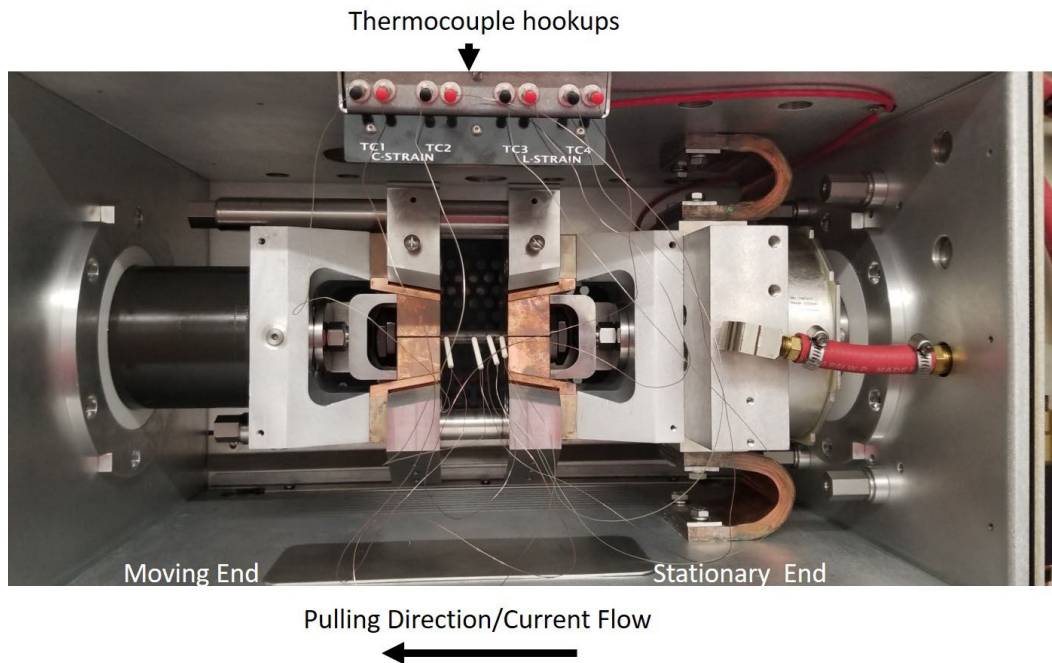


**Fig. 4** Sample using Cu grips loaded into Gleeble

After loading the sample, the test chamber was pumped down to a vacuum level of  $10^{-6}$  torr and allowed to sit there for 15–20 min. Each sample was heated to 1200 °C at a heating rate of 5, 10, or 20 °C/s and held at temperature for either 0 or 30 s before cooling. A temperature of 1200 °C was chosen to ensure that sample's microstructure would have some austenite formation before cooling (much longer hold times than 30 s are needed to ensure full transformation).<sup>5</sup> Cooling was

accomplished by having the Gleeble turn off the heating current; it was monitored for 60 s but not controlled. Finally, for each run the Gleeble was told to maintain a load of 0 kilograms of force. Data collected during the testing included the measured temperature profile of the sample, the programmed temperature profile, the power needed to heat the sample, and the load experienced by the sample during the run.

After testing, the sample that had experienced the largest thermal gradient (Sample 3 from Table 1) was sectioned, polished, and etched (2% Nital solution) via metallographic means prior to performing optical microscopy with a Keyence VHX-7100.

### 3. Results

The experimental parameters and the measured thermal gradients are included in Table 1 and Fig. 5. Sample 3 in the table had the highest measured thermal gradient and is highlighted in yellow. It was observed that the largest gradients were accomplished with the Cu grips, no hold time, and the medium heating rate.

**Table 1 Experimental parameters and measured thermal gradients; highlighted row is sample that had largest thermal gradient**

Sample number	Grip	Hold (s)	Heating rate (°C/s)	Delta T max (°C)	Thermal gradient (°C/mm)	Thermocouples used to find Delta T max	Delta T min (°C)	Thermal gradient (°C/mm)	Thermocouples used to find Delta T min
1	Cu	30	10	750	37.02	TC2–TC4	199	17.40	TC2–TC3
2	Steel	30	10	102	4.77	TC2–TC1	28	1.35	TC2–TC3
3	Cu	0	10	805.2	40.81	TC2–TC1	74.1	8.26	TC2–TC3
4	Steel	0	10	184.79	9.07	TC2–TC4	117.96	4.60	TC2–TC1
5	Cu	0	20	676.76	39.01	TC2–TC1	26.31	2.83	TC2–TC3
6	Cu	0	5	732.56	32.39	TC2–TC4	NA	NA	TC3 failed during run

Figure 5 shows the measured temperatures from each TC during the Gleeble runs in Samples 1 through 4. Because TC2 and TC3 were always close to one another, there is only a small (relative) measured temperature difference between them in each sample. Because TC1 and TC4 were always nearest to the grips (5 to 7 mm away), although on different sides of the sample, their measured temperature profiles are very similar. Their proximity to the grips meant the largest thermal gradients were always measured between TC2 and either TC1 or TC4 (Figs. 6 and 7), depending whether TC1 or TC4 was closer to a grip.

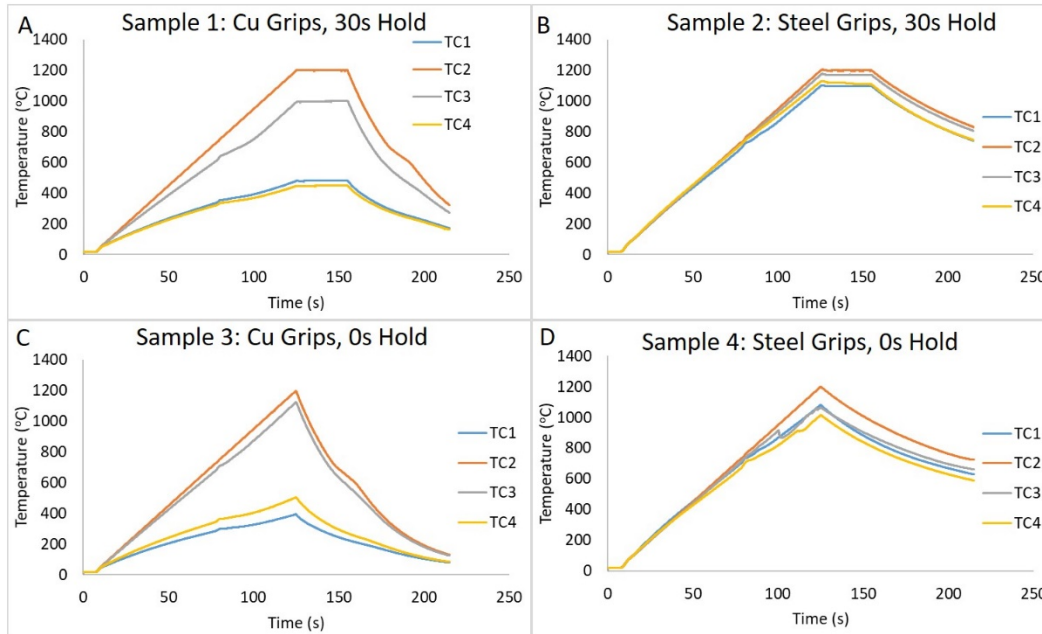


**Fig. 5 Measured temperature profiles for Samples 1–4; Sample 2 had smallest thermal gradient while Sample 3 had largest**

Figures 6 and 7 show the maximum temperature measured by each TC as a function of distance from the contact point between the sample and the grip at the stationary end of the Gleeble (Fig. 4), depending whether Cu (Fig. 6) or steel (Fig. 7) grips were used. These figures again show the gradients are largest from the ends of the sample to the center and that the gradients are much larger when the Cu grips are used rather than the steel grips. Of note, the distances are larger in Fig. 7 than in Fig. 6 because of the reduced contact area between the sample and the steel grips (Fig. 2c).

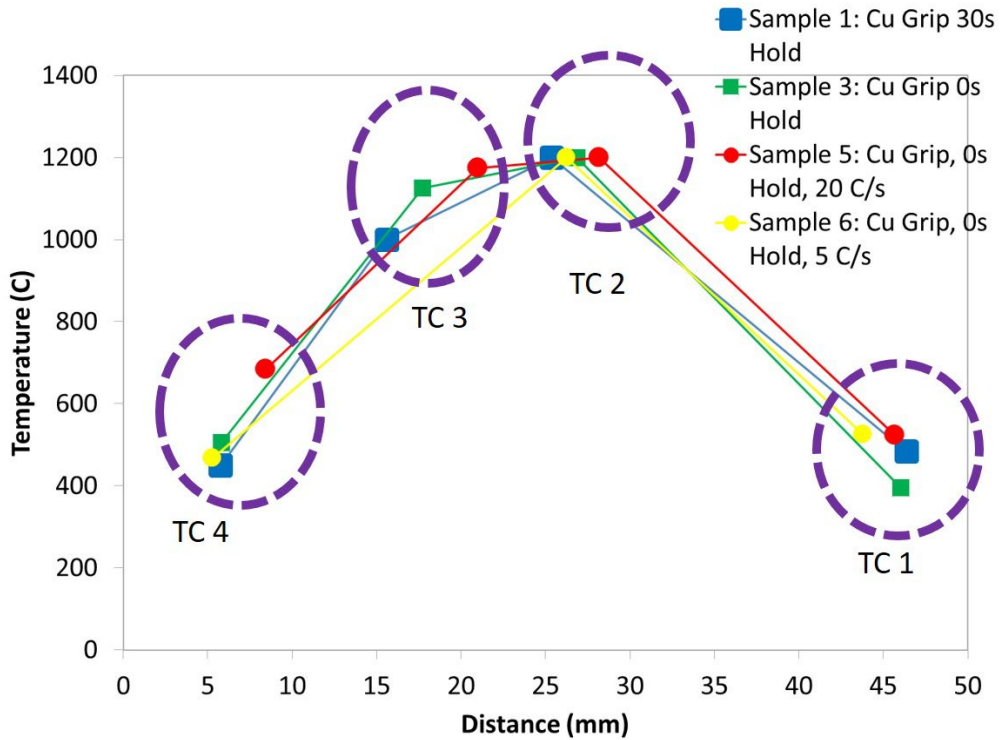


Fig. 6 Measured maximum temperatures for each TC for samples tested with the Cu grips (Samples 1, 3, 5, and 6) as a function of distance from stationary end of Gleeble

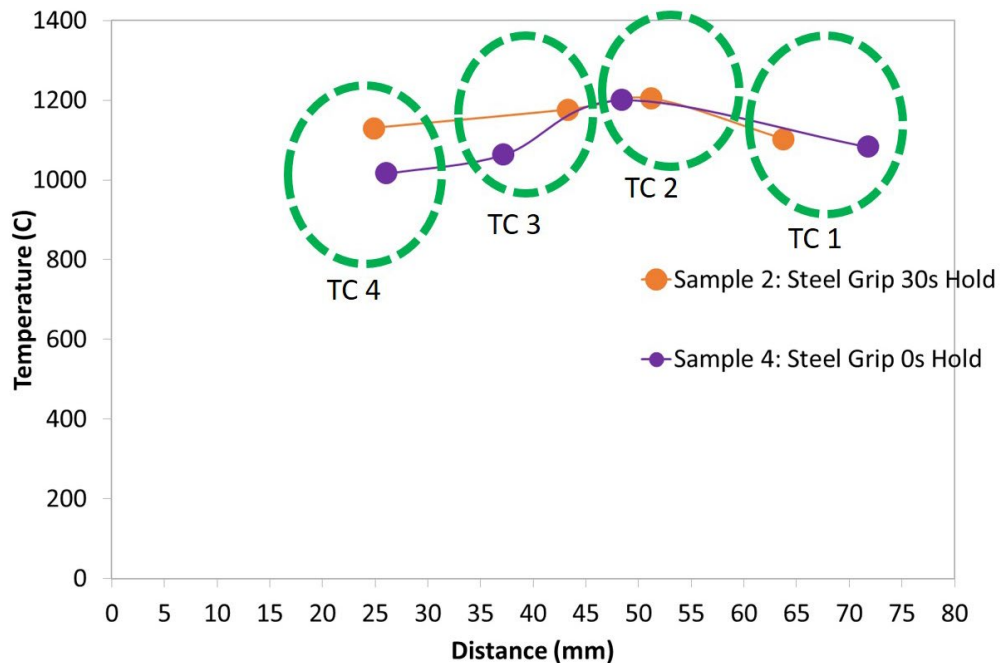
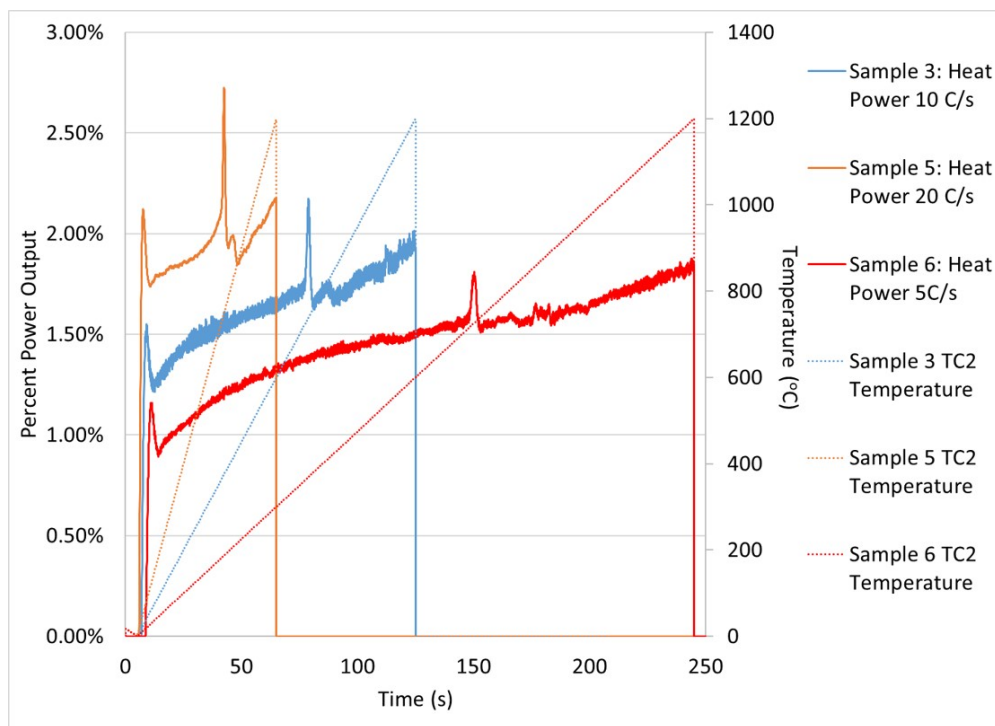


Fig. 7 Measured maximum temperatures for each TC for samples tested with steel grips (Samples 2 and 4) as a function of distance from stationary end of the Gleeble

While the influence the grips have on the size of the temperature gradients can be explained based on the differences in thermal and electrical conductivity of the two grip types, the influence of heating rate on the size of the thermal gradients is trickier to ascertain. This is seen by the fact that with heating rates of 5, 10, and 20 °C/s the middle heating rate generated the highest thermal gradients, but this may be an artifact from the duration of each run. Because these runs did not use either hold times or controlled cooling to ensure each experiment ran for the same amount of time, the duration of each experiment was different; as the heating rate doubled for each run, the duration of each run was halved. This is illustrated in Fig. 8 by overlaying the heating power output from the Gleeble during an experiment with the programmed temperature profiles for the samples with different heating rates.



**Fig. 8** Gleeble heat power (power output) as a function of time overlaid on the programmed thermal profile, as controlled by TC 2, for Samples 3, 5, and 6 run with the Cu grips, no hold time, and heating rates of 5, 10, and 20 °C/s

Figure 8 shows that without incorporating hold times or controlling the cooling rate, it is not possible to separate the influences of heating rate and experimental duration. However, as seen in Table 1 and Fig. 5, hold times can decrease thermal gradients. In theory, faster heating rates should lead to larger gradients because there is less time for the sample to reach a thermal equilibrium. However, faster heating rates in the Gleeble mean shorter test duration and less time for the gradients to develop, while slower heating rates mean less current and smaller gradients due to longer test durations allowing for equilibrium. It is probable that,

for any three chosen heating rates that are multiples of one another (i.e., 5, 10, and 20 or 3, 6, and 9), the middle heating rate, without hold times and controlled cooling, may always provide the largest thermal gradients due to a balance between power applied to the sample and test duration.

With the establishment of the thermal gradient across the sample, the next step is to figure out what the temperature is throughout the sample at points other than where direct measurements were made (i.e., at the points where there were no TCs). The easiest way to do this is with a simple curve-fitting function, such as in Excel. Using Sample 3 from Table 1, a plot of the maximum temperature measured by each TC was created and fitted with a trend line in Excel (in this case, a second-degree polynomial). The equation for the trend line can be used to solve for the temperature at any point along the curve, as illustrated in Fig. 9.\* However, for this to work there are several things to note and assumptions to make: 1) the x-axis has to be taken as distance between the TC positions and the control TC (in this case TC2) because the control TC will always be the hottest point on the sample; 2) the  $R^2$  value must be very close to 1 to assume a usable fit; 3) the control TC is at the center of the sample's gauge length; 4) the point(s) of interest within the sample fall within the section of the sample among the TCs; and 5) the sample has a uniform cross-sectional area and composition.

This is a rather simplistic approach to take, and using a more robust analytical solution (for example, a Finite Element Model) could produce more accurate results and provide a more fundamental understanding of what is occurring within the sample. Alternatively, a thermal imaging system could also be used to measure, rather than calculate the sample temperature at each point along the sample, assuming the thermal camera being used has good enough resolution.

---

\* Since TC1 was to the left of TC2 and was the only thermocouple near the moving jaw of the Gleeble (Fig. 4), it was arbitrarily given a negative distance from TC2.



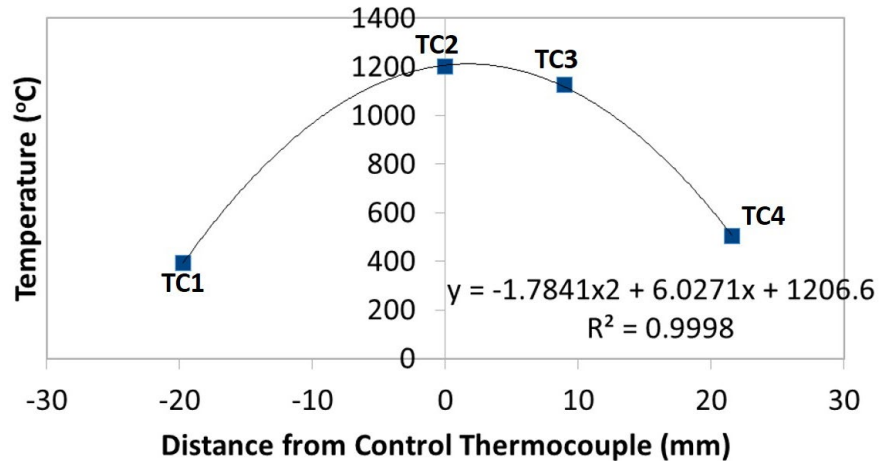


**Fig. 9** Maximum temperature measured by each TC for Sample 3 as function of distance away from control thermocouple (TC2 taken as  $x = 0$ )

Although not included here, it should be noted the data from samples where the steel grips were used was not as easily fit as the points in Fig. 9. The ease and quality of the data fit, for all samples, would be increased through the acquisition of more discrete data points (from using more TCs or from using other, additional, thermal-measurement tools) or possibly from using different distances among the TCs (either farther apart or nearer to each other).

With the establishment of a temperature–position relationship, the last step is to match the temperature–position relationship with the microstructures generated during the experimental run. Since Sample 3 had the largest thermal gradient, it was chosen as the sample to be sectioned and polished for microstructural evaluation. Figure 10 is a low-magnification image of the entire sample and has been labeled to show where in the bulk of the sample the higher-magnification images used to make Figs. 11–14 were taken.

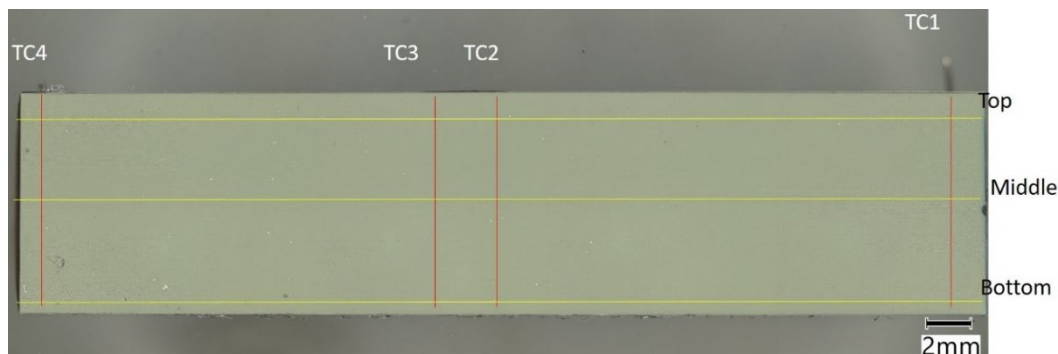


**Fig. 10** Low-magnification image of Sample 3 after metallographic preparation showing where in the sample the TCs were attached and where the higher-magnification images (Figs. 11–14) were taken

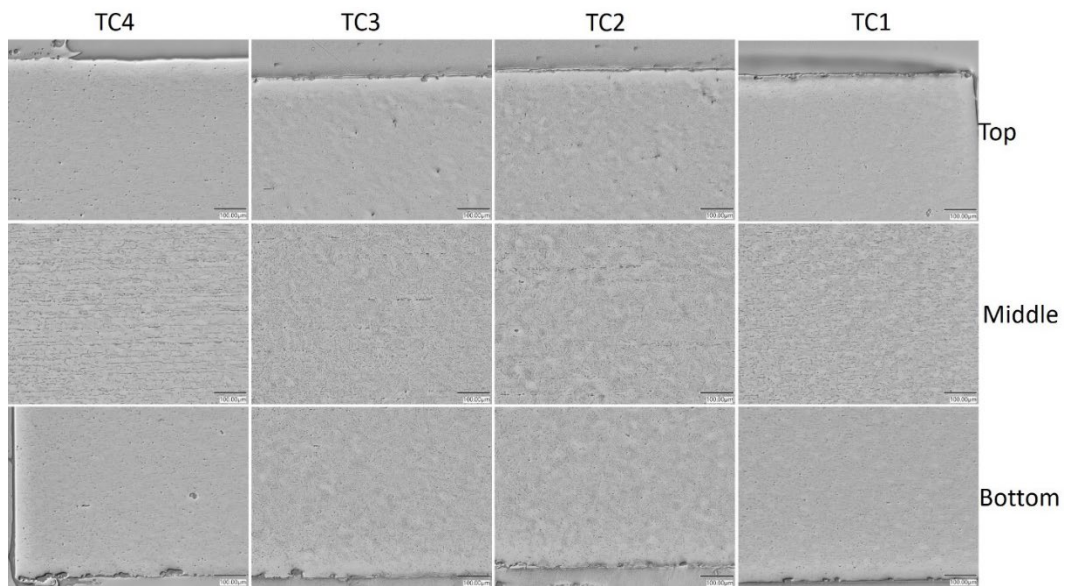


**Fig. 11 Higher-magnification images of Sample 3**

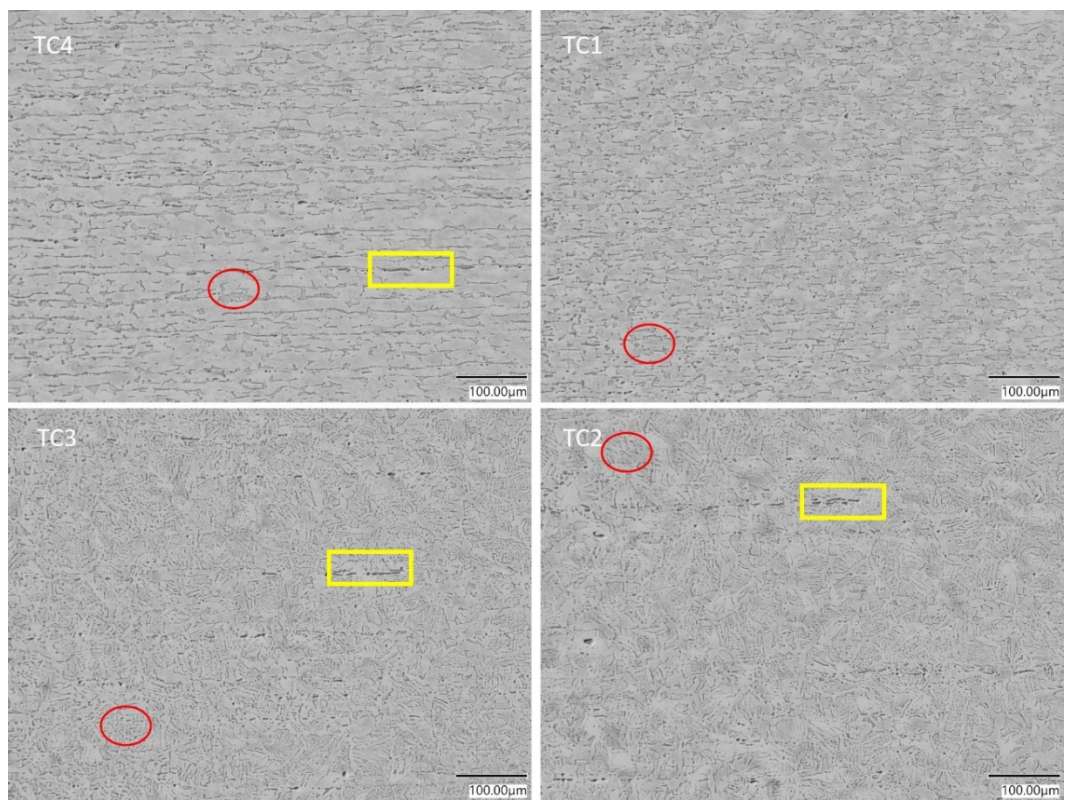


**Fig. 12 Blown-up versions of middle images in Fig. 11: yellow boxes block off precipitates seen throughout the sample while red circles are example areas of pearlite**

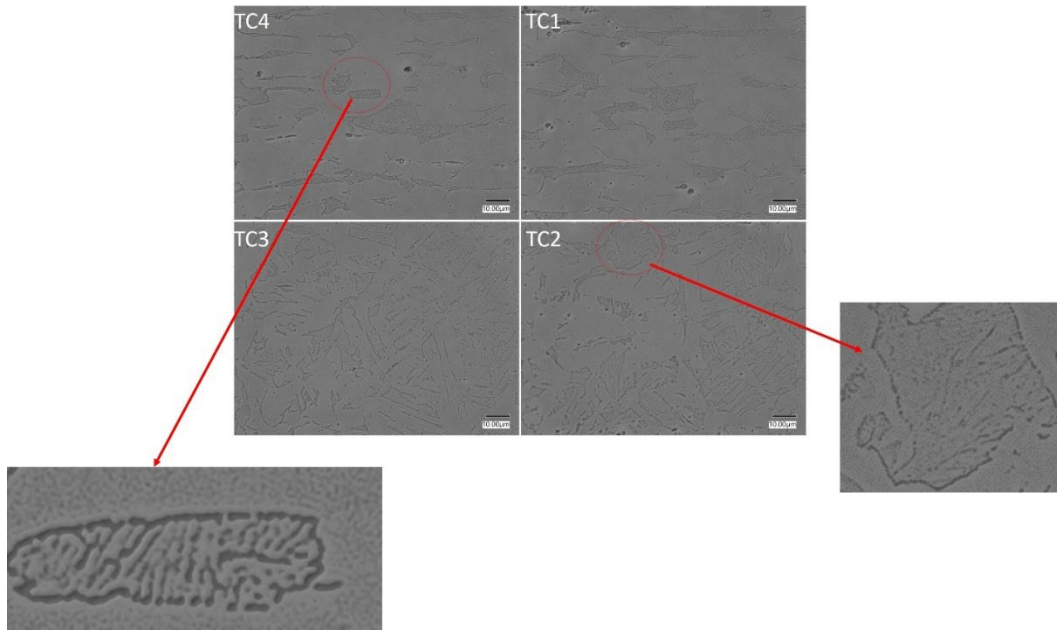


**Fig. 13** High-magnification images showing differences in the pearlite throughout sample

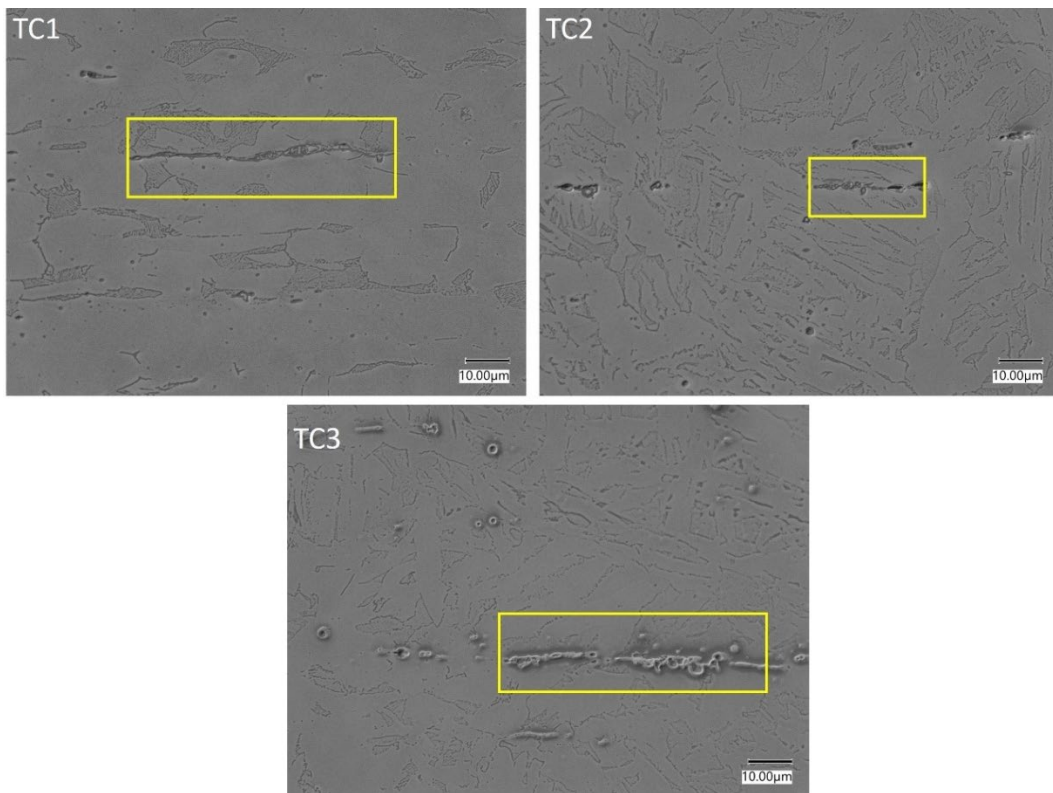


**Fig. 14** High-magnification images showing the precipitates in Fig. 12

From Fig. 11 it is evident there are different microstructures along the length of the sample (running from TC1 to TC4) but also along the radius of the sample (running

from the top of the sample to the bottom of the sample) that is made up of pearlite, ferrite, and a precipitate (most likely manganese sulfide). The microstructures on the top and bottom of the sample are the same, but look underdeveloped compared with the microstructure in the center of the sample. These differences may have been caused by various surface effects: the surface of the sample losing heat via radiation faster than the center of the sample, or the sample's surface having a slightly different chemistry due to surface oxidation. Due to these differences, the microstructural analysis is going to be based on how the microstructure in the middle section of the sample varied along the length of the sample.

Figures 12 and 13 show that the precipitates and pearlite are aligned with the ferrite grains in the regions around TC1 and TC4. However, in the higher-temperature regions (TC2 and TC3), the pearlite regions are much more randomly orientated while the precipitates appear to retain their alignment. This change in orientation may be due to the ferrite grains beginning to transform to austenite at higher temperatures (above 740 °C, Fig. 15). At higher magnification in the TC2 and TC3 regions, it appears that the pearlite phase has undergone some dissolution; had the sample been held above the eutectic (approximately 727 °C) for a longer period of time, the dissolution would have been complete. Figure 14 illustrates the precipitate phase and shows that a lot of them were pulled out during polishing. The figure also shows that they were largely unaffected by the thermal gradients.

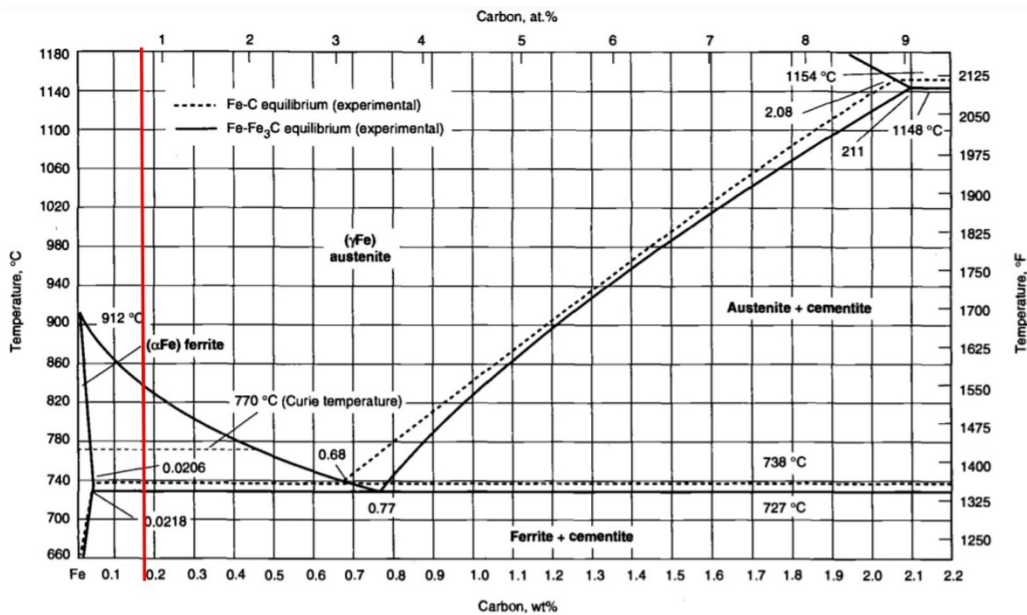


**Fig. 15** Iron-carbon phase diagram (adapted from the *Metals Handbook*<sup>5</sup>); red line roughly indicates carbon content in 1018 steel

The micrographs show how the application of thermal gradients generate multiple microstructures within a single sample work. However, the micrographs also show

more care needs to be used to properly develop these experiments. For example, a longer hold time at temperature to ensure austenite formation followed by a quench would have produced a great array of different microstructures that would have been more pertinent to material development, as opposed to the work presented here being a proof-of-concept demonstration.

#### **4. Conclusions**

---

---

While the Gleeble has been well established in industry as an important tool in alloy development, it is generally not considered a high-throughput tool as most Gleeble simulations use one sample to create one data point. Here, using 1018 steel as an example material, this report has shown how the Gleeble can contribute to HTMD through the development of microstructural libraries. After the development of these libraries, the next steps would generally be a screening of each discrete microstructure through a high-throughput method to determine mechanical properties (for example, nano-indentation) or to use advanced modeling tools to predict the behavior of each microstructure. While the 1018 steel used here was a very simple material and only produced a few, relatively simple microstructures, this method can work for any alloy system.

## 5. References

---

1. McDowell D, Olson G. Concurrent design of hierarchical materials and structures. *Sci Model Sim SMNS*. 2010;15:207–240.
2. Klitsie JB, Price AR, De Lille CSH. Overcoming the valley of death: a design innovation perspective. *Design Man J*. 2019;14-1:28–41. <https://doi.org/10.1111/dmj.12052>.
3. Introduction to high-throughput materials development. Georgia Institute of Technology; 2021. <https://www.coursera.org/learn/high-throughput>.
4. Gleeble users training 2014. Dynamic Systems Inc., 2013. p. 38–51.
5. Boyer H, Gall T, editors. *Metals handbook, desk edition*. American Society for Metals; 1992.

## List of Symbols, Abbreviations, and Acronyms

---

AC	alternating current
ARL	Army Research Laboratory
DEVCOM	US Army Combat Capabilities Development Command
DSI	Dynamic Systems, Incorporated
Cu	copper
HTMD	High-Throughput Materials Development
TC	thermocouple

1 DEFENSE TECHNICAL  
(PDF) INFORMATION CTR  
DTIC OCA

1 DEVCOM ARL  
(PDF) FCDD RLD DCI  
TECH LIB

7 DEVCOM ARL  
(PDF) FCDD RLW MD  
J LA SCALA  
P SMITH  
F KELLOGG  
C MOCK  
FCDD RLW MF  
C HAINES  
A GIRI  
FCDD RLW ME  
K BEHLER